AL-Bahir
Journal for Engineering and Pure Sciences
BJEPS

Volume 6 | Issue 2 Article 5

Preparation of Nanoparticles and Study of the Effect of Some of Their Physical Properties on Epoxy Polymer

Aya N. Abdullah
Physics Department, College of Education for Pure Science, Kirkuk University, Kirkuk, Iraq.

Niran F. Abeduljabbar
Physics Department, College of Education for Pure Science, Tikrit University, Tikrit, Iraq

Recommended Citation

Abdullah, Aya N. and Abeduljabbar, Niran F. (2025) "Preparation of Nanoparticles and Study of the Effect of Some of Their Physical Properties on Epoxy Polymer," *Al-Bahir*: Vol. 6: Iss. 2, Article 5.
Available at: https://doi.org/10.55810/2313-0083.1095

Preparation of Nanoparticles and Study of the Effect of Some of Their Physical Properties on Epoxy Polymer

Source of Funding

none

Conflict of Interest

no conflicts of interest.

Data Availability

The data supporting the findings of this study are available upon request from the corresponding author.

Author Contributions

Writing—original draft preparation, [Aya N. Abdullah]; Writing—review and editing, [Niran F. Abeduljabbar]. All authors have read and approved the final manuscript.

ORIGINAL STUDY

Preparation of Nanoparticles and Study of the Effect of Some of Their Physical Properties on Epoxy Polymer

Aya N. Abdullah [a,*], Niran F. Abeduljabbar [b]

[a] Physics Department, College of Education for Pure Science, Kirkuk University, Kirkuk, Iraq
[b] Physics Department, College of Education for Pure Science, Tikrit University, Tikrit, Iraq

Abstract

Nanoparticles were prepared by the laboratory thermal method from copper, magnesium, and zinc oxides. Different nanoparticles were added to epoxy at weight fractions of (0, 2, 4, 6, 8, 10) wt. %. The structural results from X-ray diffraction showed the appearance of epoxy in a random system, and when reinforced with nanopowders at higher addition ratios, we find the appearance of nanoparticles in a clear crystalline form, while the SEM results showed an increase in consistency and homogeneity with each increase in the proportions of nanoparticles, which appeared clearly during the EDX examination. The hardness of Shore type D was the best at 10 % for all particles, as it was (90.2HD) for (EP-10 %CuO), (88.56HD) for (EP-10 %MgO), and (87.5HD) for (EP-10 %ZnO). As for the impact resistance, magnesium oxide nanoparticles showed the best value at 10 % at (12.3 kJ/m^2). It was found that the thermal conductivity value reached its highest at the EP-10 %CuO ratio of (0.5528 W/m.K), while for the EP-10 %ZnO composite at the same concentration its value was (0.4683 W/m.K), while it was the lowest in the EP-10 %MgO composite at the same addition ratio and reached (0.0453 W/m.K). It was found that the thermal conductivity value reached its highest at the EP-10 %CuO ratio of (0.5528 W/m.K), while for the EP-10 %ZnO composite at the same concentration its value was (0.4683 W/m.K), while it was the lowest in the EP-10 %MgO composite at the same addition ratio and reached (0.0453 W/m.K).

Keywords: SEM, Thermal conductivity, Thermal method, XRD

1. Introduction

Epoxy has emerged as one of the most notable polymers due to its exceptional properties, such as electrical insulation, chemical resistance, and high stiffness [1]. During the 20th century, composite materials experienced a revolutionary transformation driven by advancements in materials science, positioning polymers as essential components in the design of engineering systems [2]. However, limitations inherent in the traditional structure of epoxy, such as susceptibility to crack propagation and subpar performance under dynamic stresses, have motivated researchers to explore methods to enhance its performance [3].

Nanomaterials possess a remarkable capacity to improve the critical properties required in industrial applications, particularly those necessitating high resistance to mechanical stresses and elevated temperatures [4]. Although polymeric materials have been widely employed across various industries, their mechanical and structural properties remain inherently weak, necessitating reinforcement with ceramic nanopowders [5]. Epoxy, known for its high tensile strength and resistance, benefits significantly from reinforcement with nanomaterials, enabling its application in industrial and medical fields [6]. Reinforcement using laboratory-prepared nanopowders, particularly via thermal methods, represents a promising industrial

Received 7 February 2025; revised 6 March 2025; accepted 6 March 2025.
Available online 11 April 2025

* Corresponding author.
E-mail addresses: ayanabel@uokirkuk.edu.iq (A.N. Abdullah), niran.fadhil64@tu.edu.iq (N.F. Abeduljabbar).

https://doi.org/10.55810/2313-0083.1095

approach. This technique strengthens the stiffness, hardness, and impact resistance of epoxy-based composites, resulting in materials with excellent and versatile polymer matrices [7].

Incorporating nanopowders of ceramic oxides, such as copper oxide, magnesium oxide, and zinc oxide, into polymeric materials, including epoxy, markedly enhances their mechanical properties, as well as their thermal and chemical stability [8]. Nanoparticles excel in filling inter-spaces within polymer chains, reducing molecular mobility, and reinforcing internal stacking between polymer and nanoparticles [9]. Consequently, composites derived from integrating nanoparticles with polymers exhibit superior structural characteristics. These materials are particularly suited for applications in aviation, space, and the automotive industry, where lightweight, high mechanical strength, and tolerance to high temperatures are critical [10].

Nonetheless, this technology is not without challenges. One notable drawback is the extended time required for nanopowder preparation through processes involving magnetic mixing, continuous stirring, and sustained heating to convert salts or nitrates into their final nano forms [11]. The thermal method, however, holds significant promise for producing nanoparticles with extensive applications. Its key advantages include low production costs, the simplicity and availability of required devices in most laboratories, and the ability to produce nanomaterials in large quantities within a reasonable timeframe [12,13]. The present study aims to explore the impact of incorporating ceramic nanopowders into epoxy at varying reinforcement ratios. It focuses on analyzing structural properties using scanning electron microscopy (SEM) and X-ray diffraction (XRD) techniques, in addition to evaluating thermal conductivity at each reinforcement level. The objective is to gain insights into the behavior of epoxy reinforced with nanoceramic powders and assess its potential for various industrial applications.

2. Raw materials and expremantal part

The base material of the composite was epoxy type (Sikadur 52) consisting of epoxy with hardener, of Egyptian origin and produced by (Sika Egypt for Construction Chemicals). The reinforcement materials were nanoparticles produced from hydrated materials nitrates, which were hydrated copper nitrate ($Cu(NO_3)_2 \cdot 3H_2O$) with a molecular weight of (241.60), hydrated magnesium nitrate ($Mg(NO_3)_2 \cdot 6H_2O$) with a molecular weight of (256.41), hydrated zinc nitrate ($Zn(NO_3)_2 \cdot 6H_2O$) with a molecular weight of (297.47), and all of these salts were produced by (Laboratory Reagent) of Spanish origin. Polyvinylpyrrolidone (PVP) type (Povidone K30) with molecular formula (C_6H_9NO)n and average molecular weight (40,000 avg.) produced by the English company (Glentham Life Sciences).

The practical side involved utilizing the thermal method to produce nanoparticles from copper, magnesium, and zinc hydrated salts. This method began by dissolving 3 g of PVP in 100 moles of deionized water using a magnetic stirrer equipped with a magnetic capsule, ensuring no heat was applied until the polymer material was fully dissolved [14]. Subsequently, 5 m mol of copper hydrated salts, equivalent to 1.28 g, were added as per Equation No. (1) below. The calculated weight of copper hydrated salts was mixed with the PVP solution at 50 °C for 1 h until complete dissolution. The magnetic capsule was then removed, the stirrer turned off, and the solution was left at 85 °C for (5–6) hours to yield a semi-glassy solid material. The resulting material was ground into powder and thermally sintered in a Korean-made Muffle oven at 600 °C for 3 h to produce ready-made nanopowder. The same steps were repeated for magnesium and zinc salts in multiple experiments to achieve the required amount of nanopowders. The subsequent step involved reinforcing the resulting powders into epoxy with specified weight fractions, ensuring the ratio of epoxy to hardener was maintained at (3:1).Equation No. (2) was employed to calculate the required weight fractions [15]. The mixing mold, designed with dimensions (10 cm × 10 cm) featuring a glass base and plastic edges, was prepared. Metal powders were incorporated into the epoxy at weight fractions of (0, 2, 4, 6, 8, 10) wt. % for each type of powder. The mixing process was continued until achieving complete homogeneity between the powders and epoxy. The resulting mixture was poured into the mold to form a layer and left undisturbed for 15 days to ensure chemical stability between the composite materials, while carefully removing any air bubbles generated during casting. After the curing period, the castings were removed and subjected to heat treatment in a thermal oven at 100 °C for 30 min. This treatment aimed to finalize the hardening process, relieve stresses, reduce moisture content, and enhance mechanical properties. The castings were then cut according to the required specifications for various tests within the practical framework. The cutting process was performed using a (CO_2 System RD) laser with a capacity of 130 Watts. The final samples, reinforced with nano copper, magnesium, and zinc oxides, are shown in Fig. 1.

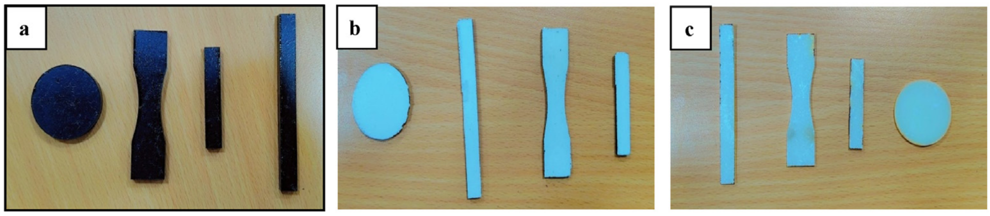

Fig. 1. Sectioned samples of (a - EP-CuO, b - EP-MgO, c - EP-ZnO).

$$Number\ of\ moles = \frac{Weight}{Molecular\ Weight} \quad (1)$$

$$w_t\% = \frac{w_p}{w_p + w_m} \times 100\ \% \quad (2)$$

w_t: The weight fraction of the reinforcement material.

w_p, w_m: Weight of the powder and base material.

3. Theoritacal part

3.1. FE-SEM and XRD test

The structural analyses were performed using scanning electron microscopy (SEM) and X-ray diffraction (XRD) to determine the particle size and identify the composition of the nanopowders used in the experimental study. The SEM analysis was conducted using a TESCAN MIRA3 microscope of French origin, while the XRD measurements were carried out with a Phillips Xpert PA Analytical system of Dutch origin. These tests were performed on all the primary powders, including CuO, MgO, and ZnO.

3.2. Hardness Shore D test

Hardness is generally defined as the resistance of a material surface to pressure applied to it, i.e. the result of force to area. Shore hardness was used because it is suitable for hard plastics as in the case of epoxy reinforced with nanomaterials. The specifications of the device used were a point drill with a diameter of (1.4 mm) and an end with a diameter of (0.1 mm) and the angle of the drill was at 30°. A pressure force is applied by the point drill on the surface of the samples, which gives a direct reading on the digital device screen, and the amount of any deviation represents the value of the scratch on the surface of the samples [16].

3.3. Impact test

In order to conduct the impact resistance test using the Charpy Test, the sample is placed horizontally and hit with a hammer with a specific weight, and the impact resistance value is calculated using equation (3) after the samples are cut into dimensions of (55 mm) in length, (10 mm) in width, and (10 mm) in height, according to the standard specifications for the impact test [17]. The test was repeated five times.

$$\mathrm{I.S} = \frac{\mathrm{E}}{\mathrm{A}} \quad (3)$$

Where: I.S: Impact strength (KJ/m^2), E: Fracture energy (KJ), A: Area of the specimen (m^2).

The fracture energy was calculated using equation (4) shown below [17]:

$$E = mgh \quad (4)$$

Where: m: Mass of the weight (kg), g: Acceleration due to gravity (9.806 m/s^2), h: Falling distance of the weight (m).

3.4. Thermal conductivity

Polymers are distinguished by their physical structure, which plays a crucial role in defining their mechanical and physical properties, such as transparency, strength, and flexibility, making them suitable for a wide range of industrial applications [18]. The internal molecular structure significantly influences the resistance of polymers to stress, melting, and decomposition under various environmental conditions, thereby reducing cracking and enhancing their stability. Thermally, polymers exhibit low thermal conductivity, making them an excellent choice for thermal insulation. Their thermal properties are determined by factors such as thermal conductivity (k), glass transition temperature (Tg), and crystal melting point (Tm), all of which influence their ability to withstand and transfer heat. In polymers, heat is transmitted through conduction, convection, and thermal radiation. The rate of heat transfer is directly proportional to the temperature difference between the hot and cold bodies (T1 < T2), a principle that is vital in designing insulation materials for various applications. The thermal conductivity of polymers is typically measured using the "Lee disk" method, as described in Equation (5) [19]. This technique involves placing the polymer sample between an electric heater and metal disks, then measuring the resulting thermal changes until a steady-state condition is achieved. The obtained data is analyzed using mathematical equations that incorporate key thermal parameters, such as temperature, thickness, and radius, to accurately assess the material's performance and optimize its properties for diverse industrial applications.

$$k\left\{\left(\frac{T_{B-}T_A}{d_s}\right)\right\} = e\left[T_A + \frac{2}{r}\left(d_A + \frac{I}{4d_s}\right)T_A + \frac{1}{2r}d_sT_B\right] \tag{5}$$

Where: e: The thermal energy per unit area of the disk per second (W/m^2. K) which can be found from equation (6) below [17,18]:

$$IV = \pi r^2 e(T_A + T_B) + 2\pi re\left[d_AT_A + d_s\left(\frac{1}{2(T_A+T_B)}\right) + d_BT_B + d_CT_C\right] \tag{6}$$

Where: (T_A, T_B,T_C): The temperatures of the three discs (A,B,C) (°C). d: Thickness of each disc (mm). r: Half of each disc (mm). I: Heating current (Ampere). V: Voltage applied to the heater (Volt).

4. Result and discussion

4.1. Scanning electron microscope testing of composite

Fig. 2 presents scanning electron microscope (SEM) images coupled with energy-dispersive X-ray (EDX) spectroscopy for the primary nanopowders, including copper oxide (CuO), magnesium oxide (MgO), and zinc oxide (ZnO). The images were captured at a scale of 10 μm, a magnification power of 5KX, and an electron beam intensity at a voltage of 7 kV. Fig. 1-a illustrates the copper oxide (CuO) nanopowder, revealing an irregular grain morphology accompanied by agglomeration and clustering of nanoparticles with rough edges. These surface clusters are primarily attributed to interactions between the surface forces of the grains [19]. Fig. 1-b displays the magnesium oxide (MgO) nanopowder, characterized by its plate-like structure with sharp grain edges. This morphology contributes to high strength and cohesion, which in turn enhances the mechanical properties of composite materials. The observed agglomeration and clustering in MgO nanoparticles can be attributed to

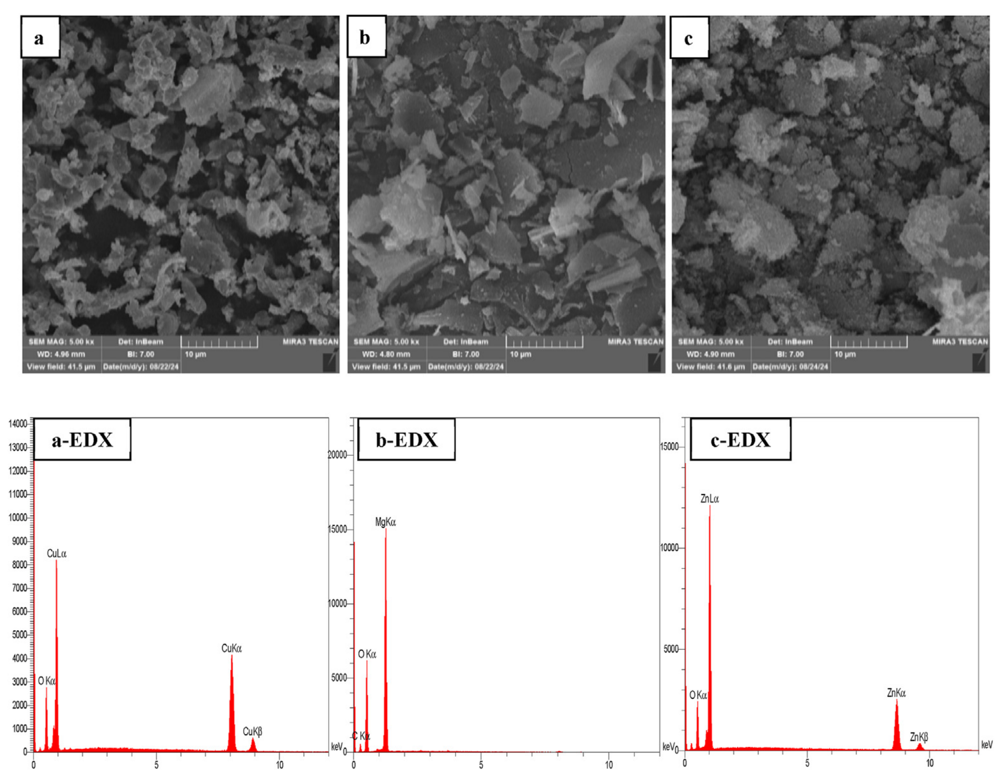

Fig. 2. Scanning Electron Microscope images (SEM) and X-ray energy spectroscopy (EDX) of the three nanopowders (a-CuO, b-MgO, c-ZnO).

their nanoscale nature [20]. Fig. 1-c shows the zinc oxide (ZnO) nanopowder, which appears in the form of semi-spherical and irregular granules, alongside evident nano-agglomeration. Such granular nano-structures are typically employed in applications requiring high stress tolerance and improved mechanical properties [21]. The EDX spectroscopy analysis of the three primary nanopowders confirms the high purity of the synthesized nanomaterials, produced via the thermal method. The absence of noticeable impurities in the spectra highlights the success of this fabrication technique in producing high-purity nanomaterials under relatively simple laboratory conditions [22,23].

Fig. 3 shows the scanning electron microscope images at different reinforcement ratios of nano-copper oxide powder (0, 2, 4, 5, 6, 8, 10) Wt. % added to the epoxy. We find that the copper oxide particles are gradually spread on the epoxy substrate with each addition. This consistency increases to reach the best crystal consistency at the ratio (EP-10 % CuO). The image highlights the integration of the particles within the polymer, with some possible agglomerations and surface defects, reflecting a homogeneous distribution of the particles within the matrix. Fig. 4 shows the scanning electron microscope images at different reinforcement ratios of nano-magnesium oxide powder (0, 2, 4, 5, 6, 8, 10) Wt. % added to the epoxy. The best scanning electron microscope (SEM) image of the sample (EP-10 % MgO) shows the distribution of magnesium oxide (MgO) particles at 10 % within the epoxy matrix (EP). The image shows a relatively homogeneous distribution of particles with a clear decrease in agglomerations, reflecting good integration of MgO particles into the polymer matrix [24]. Fig. 5 shows the SEM images at different reinforcement ratios of ZnO nanopowder (0, 2, 4, 6, 8, 10) Wt. % added to the epoxy. The best SEM image of the (EP-10 % ZnO) sample shows the distribution of 10 % ZnO particles within the epoxy matrix (EP). The image highlights the presence of clear agglomerations of particles with a rough surface, indicating a relatively heterogeneous integration of ZnO into the polymer matrix [25].

The X-ray diffraction (XRD) results for the three nanopowders—nano copper oxide, nano magnesium oxide, and nano zinc oxide—are presented in Figs. 6–8, respectively. Additionally, Tables 1–3 provide detailed data on diffraction angles, peak broadening (midpoint width), crystal size, Miller indices, and phase type for each nanopowder. Fig. 6 illustrates the X-ray diffraction pattern of nano copper oxide (CuO), which adopts a monoclinic crystal system, in accordance with the international reference card (00-901-6326). The characteristic diffraction peaks at $2\theta = 35.5°$ and $2\theta = 38.7°$ indicate a high degree of Crystallinity in the material. Table 1 further confirms the high purity of the nano copper oxide, revealing its monoclinic structure. The observed nanoscale crystal sizes, along with the sharp diffraction peaks, indicate a well-crystallized structure, contributing to superior mechanical and chemical

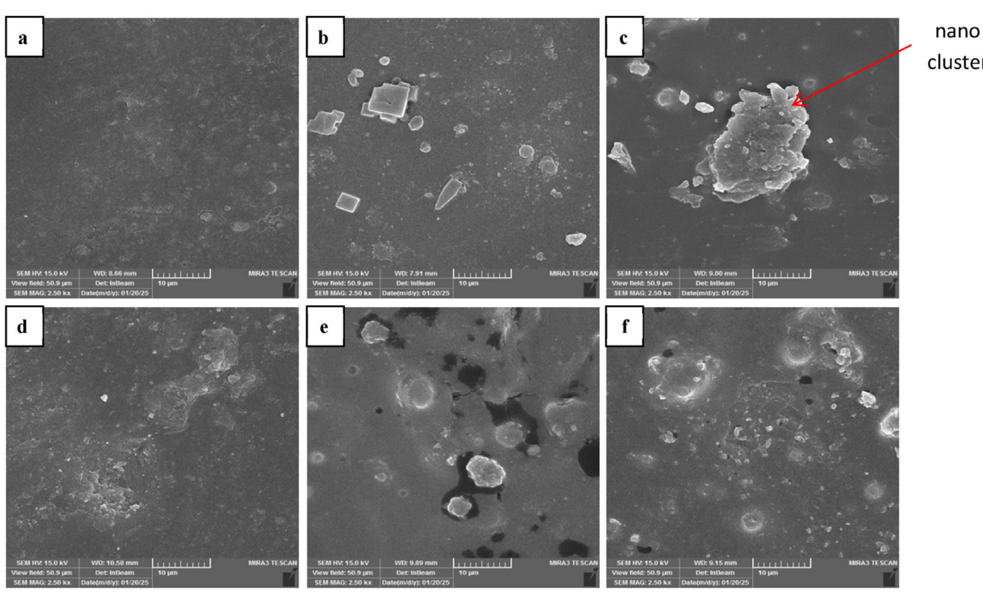

Fig. 3. Scanning electron microscope (SEM) images of (EP- %CuO) composites with different reinforcement ratios (a-0 %, b-2 %, c-4 %, d-6 %, e-8 %, f-10 %).

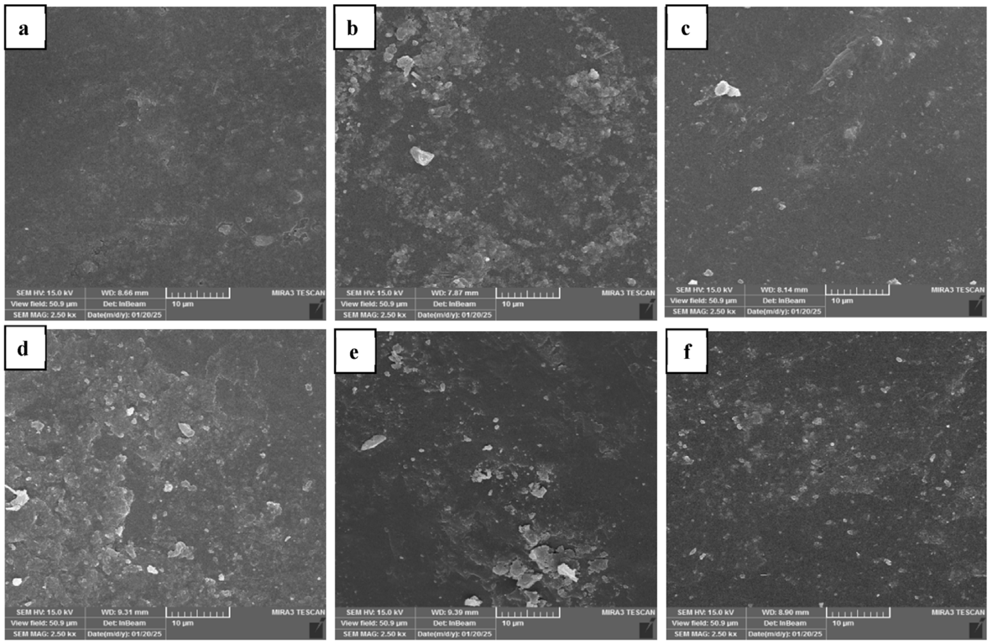

Fig. 4. Scanning electron microscope (SEM) images of (EP- %MgO) composites with different reinforcement ratios (a-0 %, b-2 %, c-4 %, d-6 %, e-8 %, f-10 %).

properties, making CuO suitable for various industrial and technical applications. Fig. 7 presents the X-ray diffraction pattern of nano magnesium oxide (MgO), where the most prominent peak corresponds to the Miller index (200) at $2\theta = 43^{\circ}$ with high sharpness. The XRD analysis confirms that nano MgO crystallizes in a cubic crystal system, as verified by its match with the international reference card (00-100-0053). The high Crystallinity of the MgO nanoparticles enhances their suitability for diverse industrial applications. Table 2 provides a precise structural analysis, indicating that the cubic crystal structure is highly ordered, with nano-scale crystal sizes ranging between 30.0 and 45.0 nm. These characteristics make nano MgO ideal for a wide array of industrial and research

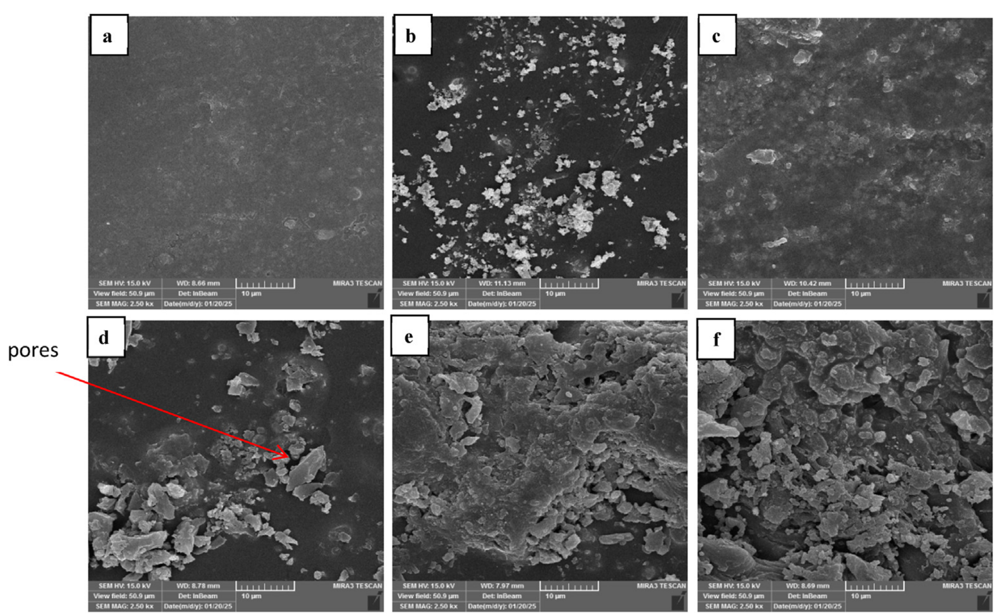

Fig. 5. Scanning electron microscope (SEM) images of (EP- %ZnO) composites with different reinforcement ratios (a-0 %, b-2 %, c-4 %, d-6 %, e-8 %, f-10 %).

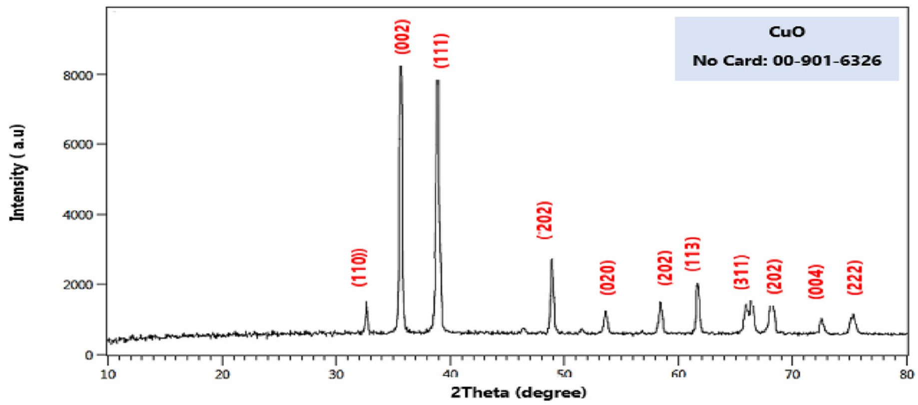

Fig. 6. X-ray diffraction of nanocrystalline copper oxide powder CuO.

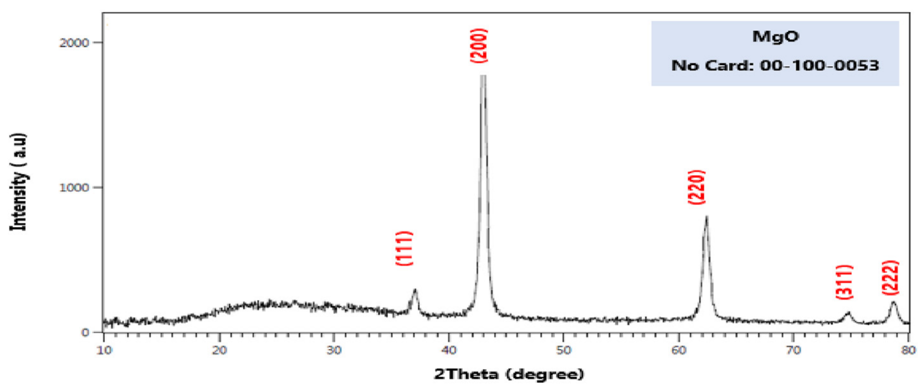

Fig. 7. X-ray diffraction of nanocrystalline Magnesium oxide powder MgO.

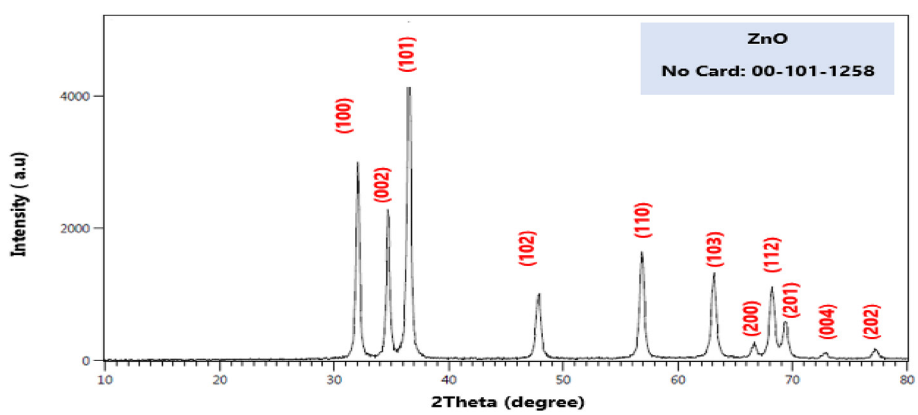

Fig. 8. X-ray diffraction of nanocrystalline zinc oxide powder ZnO.

applications. Fig. 8 displays the X-ray diffraction pattern of nano zinc oxide (ZnO), which exhibits a hexagonal crystal system, as confirmed by its alignment with the international reference card (00-101-1258). This crystal structure is typical of ZnO, with the strongest diffraction peak occurring at $2\theta = 36.3°$, corresponding to the Miller index (101). The dominance of this diffraction plane suggests that it is the most frequently occurring orientation within the hexagonal system. Table 3 confirms that nano ZnO possesses a high-purity hexagonal crystal structure with crystallite sizes ranging between 18.0 and 42.0 nm. These structural properties make ZnO highly suitable for a broad range of applications in both industrial and research domains [26–28].

Table 1. X-ray diffraction parameters of copper oxide nanopowder.

Powder	2θ (Degree)	(FWHM)	Crystal size (D)	Miller coefficients (hkl)	Phase system
CuO	32.5	0.15	42.8 nm	(110)	Monoclinic
	35.5	0.20	36.0 nm	(002)	Monoclinic
	38.7	0.18	39.5 nm	(111)	Monoclinic
	48.7	0.22	34.0 nm	(20-2)	Monoclinic
	53.5	0.25	31.5 nm	(020)	Monoclinic
	61.0	0.17	38.0 nm	(202)	Monoclinic
	66.5	0.19	37.0 nm	(113)	Monoclinic
	68.2	0.30	28.0 nm	(311)	Monoclinic
	72.5	0.35	25.0 nm	(302)	Monoclinic
	75.0	0.40	22.5 nm	(004)	Monoclinic

Table 2. X-ray diffraction parameters of Magnesium oxide nanopowder.

Powder	2θ (Degree)	(FWHM)	Crystal size (D) (D)	Miller coefficients (hkl)	Phase System
MgO	36.86	0.18	38.0 nm	(111)	Cubic
	42.9	0.15	45.0 nm	(200)	Cubic
	62.4	0.20	40.0 nm	(220)	Cubic
	74.6	0.25	35.0 nm	(311)	Cubic
	78.6	0.30	30.0 nm	(222)	Cubic

Table 3. X-ray diffraction parameters of zinc oxide nanopowder.

Powder	2θ (Degree)	(FWHM)	Crystal size (D)	Miller coefficients (hkl)	Phase System
ZnO	31.8	0.20	39.0 nm	(100)	Hexagonal
	34.4	0.18	42.0 nm	(002)	Hexagonal
	36.3	0.25	34.0 nm	(101)	Hexagonal
	47.5	0.22	36.5 nm	(102)	Hexagonal
	56.6	0.30	30.0 nm	(110)	Hexagonal
	62.9	0.35	28.0 nm	(103)	Hexagonal
	66.21	0.36	26.62	(200)	Hexagonal
	68.0	0.40	25.0 nm	(112)	Hexagonal
	69.1	0.45	22.0 nm	(201)	Hexagonal
	72.4	0.50	20.0 nm	(004)	Hexagonal
	76.0	0.55	18.0 nm	(202)	Hexagonal

4.2. Shore hardness affected by changing reinforcement ratios

The hardness test of type (Shore D) was conducted for epoxy before and after reinforcement with nanoparticles at different weight percentages (0 %, 2 %, 4 %, 6 %, 8 %, 10 %) of (CuO, MgO, ZnO) as shown in Fig. 9, to study the effect of the weight percentage of reinforcement on the hardness of pure and reinforced epoxy. The results showed that the hardness of pure epoxy increases significantly when reinforced with nanoparticles, and increases further with increasing the weight percentage of reinforcement. This improvement is due to the nature of the nanoparticles in terms of shape, size and hardness, and to their easy penetration between the spaces between the polymer chains, which leads to increased compactness of these chains and reduced their movement, thus increasing the hardness of the prepared material. The results also showed that the composite reinforced with CuO (EP-CuO) has slightly higher hardness values compared to other composites [29]. This can be explained by the viscosity of the polymer composite melt and the high homogeneity between the matrix and the reinforced nanoparticles, which reduces the penetration of the liquid matrix into the pores and interstitial spaces in the composite, thus increasing the hardness of the material. On the other hand, the concept of hardness is a measure of the resistance of a material to plastic deformation caused by external stress. Since ceramic nanoparticles such as CuO have high hardness, their addition to the epoxy increases the hardness of the material due to the improvement of its resistance to plastic deformation. This explains the gradual increase in hardness with increasing the weight percentage of reinforcement [30]. For the EP-MgO and EP-ZnO composites, they showed the lowest hardness values compared to the other composites. This difference in hardness is due to the nature of zinc oxide (ZnO), which has a relatively lower hardness compared to MgO, CuO [31]. In addition, increasing the weight percentage of reinforcement reduces the percentage of the base material within the composite material, which weakens the bond between the reinforcement material and the base material, thus reducing the positive effect on the hardness of the material [32].

4.3. Impact test affected by variable nano-additions

The effect of rapid and static stresses on composite materials such as epoxy resin was studied as shown in Fig. 10 which gives the relationship between impact strength and variable nanoparticle addition ratios, where the results showed that the material exhibits ductile behavior under static stresses, but appears brittle under rapid stresses. The impact strength of pure epoxy reinforced with nanoparticles was studied using the Charpy Impact Test to determine the absorbed energy required for fracture when adding nanoparticles at different weight ratios (0 %, 2 %, 4 %, 6 %, 8 %, 10 %) of CuO, MgO, ZnO. The results showed that the absorbed energy required for fracture of pure epoxy increases significantly after reinforcement with nanoparticles, which led to a significant improvement in impact strength. In the case of pure epoxy, failure occurs due to the breakdown of bonds between polymer chains as a result of the rapid growth of initial cracks towards the surface, as these bonds depend on van

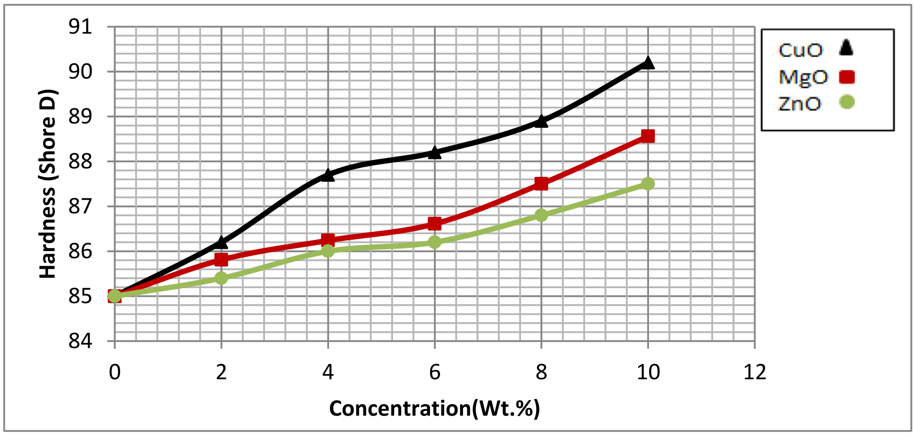

Fig. 9. The relationship between hardness Shore D and the variable proportions of nano-additions.

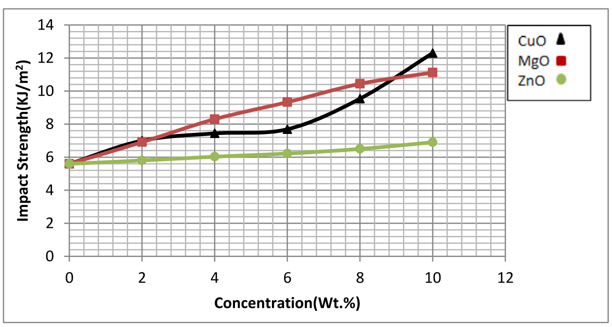

Fig. 10. The relationship between impact strength and the variable proportions of nano-additives.

der Waals forces that require low energy to overcome [33]. However, when epoxy is reinforced with nanoparticles, these particles contribute to the stress tolerance and prevent crack growth within the material, which increases the impact toughness. Increasing the weight percentage of nanoparticles enhanced the mechanical properties of epoxy by reducing the gaps and dislocations that form during the forming process. The physical and chemical interaction between the reinforcement and matrix material also significantly improved the internal bonding and increased the material's ability to withstand stresses. Moreover, the nanoparticles act as strong stress centers that hinder crack propagation, which increases the material's strength [34]. The results showed that the impact toughness varies depending on the type of nanoparticles used. The composite reinforced with (EP-CuO) recorded the highest impact toughness values, thanks to the strong interfacial bonding and physical and chemical interaction between CuO and epoxy [35]. CuO nanoparticles, due to their ceramic nature, have high stress resistance and significantly improve the mechanical properties. In contrast, the composite reinforced with (EP-MgO) recorded the lowest impact toughness values, indicating that the interfacial interaction between MgO and the matrix is less strong compared to CuO, while the (EP-ZnO) composite had the lowest among the composites. Based on the results, it can be concluded that nanoparticle

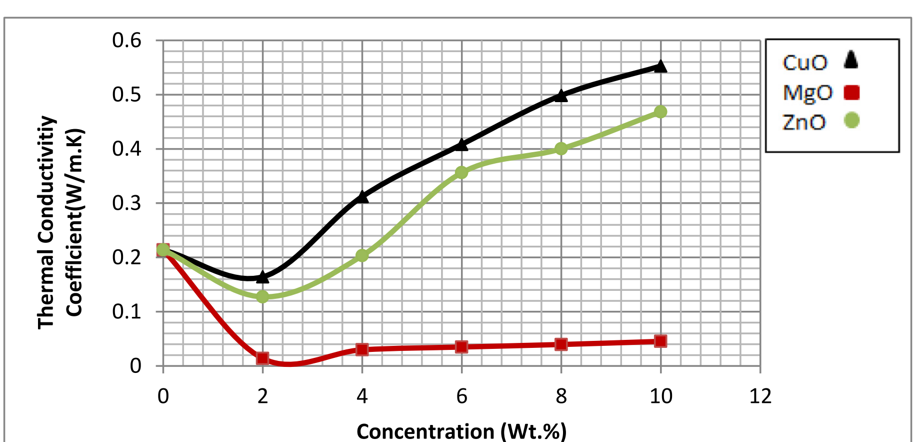

Fig. 11. The relationship between the percentages of different nano-additives (EP- %CuO, %MgO, %ZnO) and thermal conductivity.

reinforcement is an effective way to improve the impact toughness of epoxy, especially when using nanoparticles such as CuO that contribute significantly to strengthening the material and preventing crack propagation. These results highlight the importance of selecting the appropriate type of nanoparticles and focusing on improving the interfacial bonding to achieve superior mechanical properties in composite materials [36,37].

4.4. Effect of different nano additives on thermal conductivity values

Fig. 11 shows the effect of adding nanopowders of copper (CuO), magnesium (MgO), and zinc (ZnO) oxides on the thermal conductivity of epoxy at different reinforcement ratios (0 %, 2 %, 4 %, 6 %, 8 %, and 10 %). The figure shows that copper oxide (CuO) is the most efficient in improving the thermal conductivity, as the thermal conductivity coefficient increases significantly with increasing reinforcement ratio, thanks to its high thermal conductivity and good integration of particles within the polymer matrix, which forms an effective thermal network. Zinc oxide (ZnO) shows average performance, as the thermal conductivity coefficient gradually improves with increasing concentration, but it is less efficient than CuO due to its larger energy gap and different physical properties [38,39]. In contrast, magnesium oxide (MgO) shows poor performance, with a decrease in thermal conductivity at low ratios (0–2 %) and stabilization at low values with increasing concentration, which is attributed to its poor thermal conductivity and ineffectiveness in forming a thermal network within the polymer [31]. In general, the figure shows that the improvement of thermal conductivity depends on the intrinsic properties of oxides, with CuO being the most efficient choice in improving the thermal performance of polymer [40].

5. Conclusions

The results of this study demonstrate that the incorporation of nano-sized CuO, MgO, and ZnO significantly affects the microstructure, mechanical properties, and thermal performance of epoxy composites. SEM and EDX analyses confirmed the high purity of the nanopowders and their integration within the epoxy matrix, with CuO exhibiting the most uniform distribution, followed by MgO, while ZnO showed the highest degree of agglomeration. The hardness increased with higher reinforcement ratios, with CuO-reinforced composites (EP-CuO) exhibiting the highest values due to strong interfacial bonding, whereas MgO and ZnO composites had relatively lower hardness. Impact strength tests revealed that EP-CuO displayed the highest toughness, effectively preventing crack propagation, while EP-ZnO exhibited the lowest impact resistance. Thermal conductivity improved significantly with CuO, making it the most efficient thermal enhancer among the tested materials. ZnO showed moderate thermal performance, whereas MgO had the least impact on thermal conductivity. These findings confirm that nanoparticle reinforcement is an effective strategy for enhancing epoxy composites, with CuO emerging as the optimal additive for applications requiring superior mechanical strength and thermal performance. Future research should focus on optimizing nanoparticle dispersion and exploring hybrid nanofillers to achieve enhanced multifunctional properties.

Ethical Approval

None.

Source of Funding

None.

Conflict of Interest

No conflicts of interest.

Data Availability

The data supporting the findings of this study are available upon request from the corresponding author.

Author Contributions

Writing—original draft preparation, [Aya N. Abdullah]; Writing—review and editing, [Niran F. Abeduljabbar]. All authors have read and approved the final manuscript.

Acknowledgments

I would like to express my sincere gratitude and deep appreciation to my husband, Asst. Prof. Dr. Salih Younis Darweesh, for his unwavering support and encouragement throughout the preparation of this research paper. His insightful corrections and valuable suggestions have greatly contributed to enhancing the quality of this work.

References

[1] Mi X, Liang N, Xu H, Wu J, Jiang Y, Nie B, et al. Toughness and its mechanisms in epoxy resins. Prog Mater Sci 2022;130: 100977.

[2] Shubham, Ray BC. Introduction to composite materials. In: Fiber reinforced polymer (FRP) composites in ballistic protection: microstructural and micromechanical perspectives. Singapore: Springer Nature Singapore; 2024. p. 1–20.
[3] Awaja F, Zhang S, Tripathi M, Nikiforov A, Pugno N. Cracks, microcracks and fracture in polymer structures: formation, detection, autonomic repair. Prog Mater Sci 2016;83:536–73.
[4] Meyers MA, Mishra A, Benson DJ. Mechanical properties of nanocrystalline materials. Prog Mater Sci 2006;51(4):427–556.
[5] Rathod VT, Kumar JS, Jain A. Polymer and ceramic nanocomposites for aerospace applications. Appl Nanosci 2017;7: 519–48.
[6] Silvestre J, Silvestre N, De Brito J. An overview on the improvement of mechanical properties of ceramics nanocomposites. J Nanomater 2015;2015(1):106494.
[7] Shirvanimoghaddam K, Balaji KV, Yadav R, Zabihi O, Ahmadi M, Adetunji P, et al. Balancing the toughness and strength in polypropylene composites. Compos B Eng 2021; 223:109121.
[8] Moradpoor H, Safaei M, Mozaffari HR, Sharifi R, Imani MM, Golshah A, et al. An overview of recent progress in dental applications of zinc oxide nanoparticles. RSC Adv 2021; 11(34):21189–206.
[9] Ghazal NA, Majeed ZN, Darweesh SY. The effect of adding different percentages manganese on some mechanical and magnetic properties of composite (Al-Cu). AIP Conf Proc 2024, March;2885(1). AIP Publishing.
[10] Wu C, Wang Q, Wang X, Sun S, Wang Y, Wu S, et al. Al2O3 nanoparticles integration for comprehensive enhancement of eutectic salt thermal performance: experimental design, molecular dynamics calculations, and system simulation studies. Energy 2024;292:130567.
[11] Terna AD, Elemike EE, Mbonu JI, Osafile OE, Ezeani RO. The future of semiconductors nanoparticles: synthesis, properties and applications. Mater Sci Eng, B 2021;272:115363.
[12] Dahham AT, Jassim TQ, Darweesh SY. Study the effect of adding nano-magnesium oxide on some structural and mechanical properties of (Cu-10 % Fe). AIP Conf Proc 2023, December;2977(1). AIP Publishing.
[13] Karim AS, Majeed ZN, Darweesh SY. The effect of nanostructured zirconia reinforcement on the mechanical and structural properties of a copper-based system. Mater Sci Forum 2021, August;1039:297–306. Trans Tech Publications Ltd.
[14] Cao H, Jian X, Zhang D, Ling W, Zhang G, Zhang Y, et al. Amphiphilicity-driven octaphenyl polyoxyethylenes regulate soft microcapsules flexibility for better foliar adhesion and pesticide utilization. Adv Agrochem 2024;3(4):316–27.
[15] Lortholary A, Largillier R, Weber B, Gladieff L, Alexandre J, Durando X, et al. Weekly paclitaxel as a single agent or in combination with carboplatin or weekly topotecan in patients with resistant ovarian cancer: the CARTAXHY randomized phase II trial from Groupe d'Investigateurs Nationaux pour l'Etude des Cancers Ovariens (GINECO). Ann Oncol 2012;23(2):346–52.
[16] Wiley. Characterization and analysis of polymers. John Wiley & Sons; 2008.
[17] Yahya MM, Aleabi SH. Improvement some mechanical properties (impact strength, hardness, tensile strength) and thermal conductivity for epoxy coating. AIP Conf Proc 2024, March;2885(1). AIP Publishing.
[18] Lin Y, Huang X, Chen J, Jiang P. Epoxy thermoset resins with high pristine thermal conductivity. High Volt 2017;2(3):139–46.
[19] Fu YX, He ZX, Mo DC, Lu SS. Thermal conductivity enhancement with different fillers for epoxy resin adhesives. Appl Therm Eng 2014;66(1–2):493–8.
[20] Ahmed MN, Daham NA, Darweesh SY. Structural and mechanical properties for (Ni-WC) system by using thermal spray. AIP Conf Proc 2024, March;2885(1). AIP Publishing.
[21] Dong R, Gong W, Guo Q, Liu H, Yu DG. Synergistic effects of radical distributions of soluble and insoluble polymers within electrospun nanofibers for an extending release of ferulic acid. Polymers 2024;16(18):2614.
[22] Salih EJ, Allah SMA, Darweesh SY, Mohammed HA. Study of some of the physical variables of a metal-based system using the powder method. J Phys 2021, September;1999(1): 012068. IOP Publishing.
[23] Almuqrin AH, Sayyed MI, Khandaker MU, Aloraini DA, Rashad M, Elsafi M. Effect of concentration of CuO on radiation shielding characteristics of Epoxy-resin materials. Radiat Phys Chem 2024:111918.
[24] Yaseen M, Khan A, Humayun M, Bibi S, Farooq S, Bououdina M, et al. Fabrication and characterization of CuO–SiO2/PVA polymer nanocomposite for effective wastewater treatment and prospective biological applications. Green Chem Lett Rev 2024;17(1):2321251.
[25] Salih WA, Allah SMA, Darweesh SY. Effect of spray angle on some physical properties of a ceramic system produced by thermal spraying coating. Al-Bahir J Eng Pure Sci 2023;2(2):4.
[26] Humeedi SH, Shafeek NA, Ahmeed HH, Darweesh SY. The effect of adding titanium nanoparticle oxide on the physical properties of nickel by powder method. J Phys Conf 2020, November;1664(1):012078. IOP Publishing.
[27] Ota S, Harada M. Thermal conductivity enhancement of liquid crystalline epoxy/MgO composites by formation of highly ordered network structure. J Appl Polym Sci 2021; 138(19):50367.
[28] Salahuddin NA, El-Kemary M, Ibrahim EM. High-performance flexible epoxy/ZnO nanocomposites with enhanced mechanical and thermal properties. Polym Eng Sci 2017; 57(9):932–46.
[29] Vyhnánková M, Hodul J, Bydžovský J. Epoxy resin coatings crystallization and influence of crystallinity on shore hardness and tensile properties. Solid State Phenom 2018;276: 173–8.
[30] Rasheed ZN. Study of the effect of the variation effect of water temperatures on shore (D) hardness for some polymers. Al-Nahrain J Sci 2013;16(3):110–8.
[31] Mustafa A, Aloyaydi B, Sivasankaran S, Al-Mufadi FA. Shore hardness characterization of FDM printed PLA/Epoxy/MGFs composite material structure. In: Recent advances in manufacturing processes and systems: select proceedings of RAM 2021. Singapore: Springer Nature Singapore; 2022. p. 919–26.
[32] Natrayan L. and Al2O3 nanofillers epoxy hybrid composites. In: Sustainable structural materials: from fundamentals to manufacturing, properties and applications. vol. 275; 2025.
[33] Soudagar MEM, Bashir MN, Vijayan DS, Hossain I, Kannan S, Al Obaid S, et al. Study of antimicrobial and mechanical behaviors on kapok fiber reinforced bran particulates blended epoxy matrix composite. Therm Sci Eng Prog 2025;57:103123.
[34] Boulebnane A, Djeghader D, Tioua T. Weibull analysis of Charpy impact test in short date palm fiber reinforced epoxy composite. Period Polytech Civ Eng 2024;68(1):122–30.
[35] Öztaş B, Korkmaz Y, Çelik Hİ. Image analyses of artificially damaged carbon/glass/epoxy composites before and after impact load. Heliyon 2024;10(4):e25876.
[36] Xin Y, Yan H, Cheng S, Li H. Drop weight impact tests on composite sandwich panel of aluminum foam and epoxy resin. Mech Adv Mater Struct 2021;28(4):343–56.
[37] Ibraheem AM, Allah SMA, Darweesh SY. Enhancement the properties of aluminum by adding boron carbide by the powder method. J Phys Conf 2021, September;1999(1):012074. IOP Publishing.
[38] Antar RS, Darweesh SY, Ridha FW. Production of a double cermet coating to treatment of the turbine blades. Eng Res Express 2024;6(1):015407.
[39] Humeedi SH, Abdulkareem SM, Darweesh SY. The synthetic and mechanical properties of a silica matrix cermet composite. J Wuhan Univ Tech Mater Sci Ed 2022;37(3): 423–8.
[40] Cheng P, Chen X, Gao H, Zhang X, Tang Z, Li A, et al. Different dimensional nanoadditives for thermal conductivity enhancement of phase change materials: fundamentals and applications. Nano Energy 2021;85:105948.